PROCEEDINGS OF SCIENCE

# A comparison of Wilson and twisted mass valence quarks for charmed semileptonic form factors

**Julien Frison,**[a,*] **Alessandro Conigli,**[b] **Gregorio Herdoïza**[b] **and Carlos Pena**[b]

[a] *ZPPT/NIC, DESY Zeuthen, Platanenallee 6, 15738 Zeuthen, Germany*

[b] *Instituto de Física Teórica UAM-CSIC, c/ Nicolás Cabrera 13-15, Universidad Autónoma de Madrid, 28049 Madrid, Spain*

*E-mail:* julien.frison@desy.de

We present two calculations of heavy quark physics, with respectively non-perturbatively improved Wilson and twisted mass Wilson fermions, both on $N_f = 2 + 1$ CLS configurations with open boundary conditions. We evaluate those discretisations through a Ward identity on the three-point functions. We also check the universality of our continuum results. All our results are compatible with an $O(a^2)$ scaling for both actions.

*The 39th International Symposium on Lattice Field Theory,*
*8th-13th August, 2022,*
*Rheinische Friedrich-Wilhelms-Universität Bonn, Bonn, Germany*

*Speaker





PoS(LATTICE2022)408

## 1. Introduction

The Standard Model contains a considerable amount of flavour structure. Most of its parameters are related to flavour in one way or another, and their values are fundamentally unexplained. Heavy flavour physics in particular is a promising direction for the search of physics beyond the Standard Model. In many of the related processes the flavour changes occur inside hadrons, requiring a non-perturbative computation. Lattice QCD is a very attractive solution for these calculations, but, with such a high energy scale, keeping the cutoff effects under control remains a challenge.

In previous proceedings[1] [2] [3] [4] [5] [6] [7] [8], we proposed a strategy to compute heavy quark observables with twisted masses in the valence to reduce the discretisation effects. Some preliminary results have already been presented, but no data was available to make a direct comparison of the discretisation effects between this partially quenched setup and the unitary improved Wilson action. While it is clear that the mixed action should outperform an unimproved Wilson action, it could be that the improved Wilson action performs just as well.

Here, we put together a subset of data generated by two different heavy-quark calculations which both compute semileptonic form factors (as well as leptonic decays). Both calculations use the $N_\mathrm{f} = 2+1$ O(a)-improved Wilson configurations from the CLS initiative, and the selected subset focuses on the symmetric line $m_{ud} = m_s$ with heavy quarks close to the physical charm mass.

## 2. Presentation of the projects

### 2.1 Ensembles and contractions

We present in Tab. 1 the ensembles used here, on which contractions are performed according to Fig. 1. The contraction strategy is the same for both Wilson and twisted mass observables, so that only the parameters (physical or algorithmic) change. Both inversions are performed by our `openQCD`-based code, `tm_mesons`, which in particular adds distance preconditionning[9] to the SAP-GCR algorithm.

To put things in their context, we then present separately in the next subsections each of the two projects and its objectives.

| id | $\beta$ | $a^{-1}$[fm] | $N_\mathrm{s}$ | $N_\mathrm{t}$ | $m_\pi$[MeV] | $m_K$[MeV] | $m_\pi L$ | $a\mu_c$ |
|---|---|---|---|---|---|---|---|---|
| H101 | 3.40 | 0.086 | 32 | 96 | 420 | 420 | 5.8 | 0.22 |
| H400 | 3.46 | 0.075 | 32 | 96 | 420 | 420 | 5.2 | 0.21 |
| N202 | 3.55 | 0.064 | 48 | 128 | 420 | 420 | 6.5 | 0.18 |
| N300 | 3.70 | 0.050 | 48 | 128 | 420 | 420 | 5.1 | 0.14 |

**Table 1:** Ensembles considered in this proceedings, where we have analysed both Wilson and twisted mass observables. Other results are available with lighter pions, different volumes or different heavy masses, but usually not for both calculations at the same time. Open boundary conditions are applied to all ensembles to allow for finer lattice spacings.

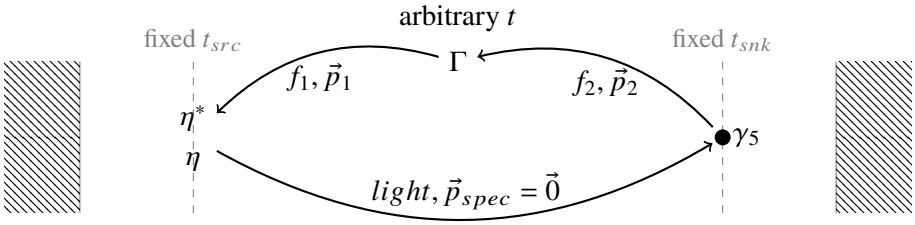


**Figure 1:** Contractions for the three-point functions related to D semileptonic decays. The one-hand-trick is one on the noise $\eta$ and the spectator quark serves as a source in a sequential propagator.

### 2.2 The twisted project

When trying to reach charm physics with a relativistic action, discretisation effects are expected to be the most challenging systematic effect. With Wilson quarks it includes in particular large $O(am_c)$ terms. Those disappear at maximal twist, as well as all even powers.

This computation therefore tries to improve the continuum limit with the introduction of a twist in the valence. Wilson fermions are kept in the valence, since no $O(am_c)$ effects can arise from $N_\mathrm{f} = 2 + 1$ configurations.

The most obvious benefit of this is that those configurations do not need to be regenerated. Instead, one needs to dedicate some effort to matching the two actions along a given continuum trajectory: for each ensemble the masses are tuned so that the PCAC mass vanishes and the meson masses correspond to the unitary action. The interpolated quark masses are used as an input for the results presented here.

Since this partial quenching only modifies the mass parameters (even the $c_{sw}$ term is kept), no new renormalisation factors are needed.

### 2.3 The Wilson step-scaling project

Another approach consists in avoiding the direct computing of observables and building ratios within a step-scaling strategy[13–15]. Various volumes are used so that one can connect computations with heavy quarks in small volume to computations with moderately heavy quarks in larger volumes.

This is what we are doing in the second calculation whose data is used here, but it is *not* the way we present this data in the present proceedings. Instead we here only consider the calculation which sits at the $L_\infty$ end of the step-scaling chain, and look at its continuum limit *before* taking any ratio. This is simply because we want a direct comparison to the twisted mass results.

It should be noted that the normalisation pattern is more complicated here, and many improvement coefficients are needed. Fortunately many non-perturbative calculations already exist as part of the ALPHA program.

## 3. Checks on some first results

### 3.1 The dispersion relation

A natural first check is the dispersion relation of pions. Indeed, we want to study the form factors on some range of momentum tranfer.

As shown in Fig. 2, both discretisations are to a large extent compatible with the continuum dispersion relation within error bars, up to the charm mass and even beyond.

Note that this is a spectral quantity and therefore no improvement coefficient is needed yet, except $c_{sw}$ or maximal twisting. Also, it is worth noting that these energies are not directly needed to compute form factors: substituting those with the continuum formula usually gives a better signal and does not change anything to the power-counting.

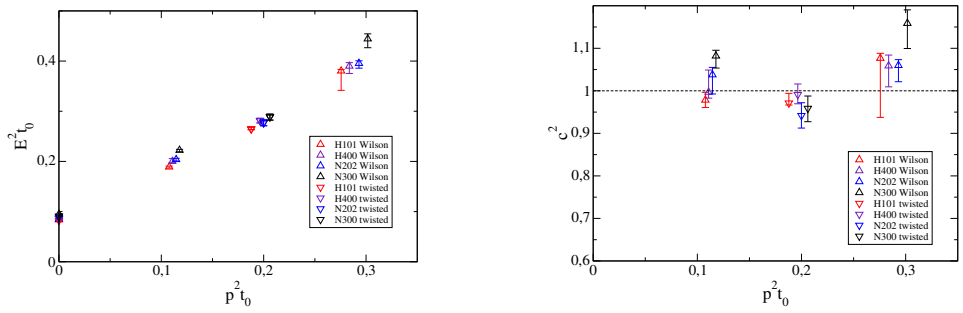


**Figure 2:** We show the pion energies $E^2 = m^2 + p^2 + O(a^2)$ on the left, and on the right we transform the same data into the speed of light $c^2 = (E^2 - m^2)/p^2 = 1 + O(a^2)$. The plateaus are averaged as in Sec. 4.2. Some intriguing tension appears for the finest ensemble, but what is more relevant for this check is that we do not observe any degradation of the agreement with the continuum relation on coarser ensembles.

### 3.2 Vector Ward identity

From the three-point functions with various current insertions, let us define, similarly for both discretisations:

$$\Delta^{tw}(t) \equiv \delta\mu C_S^{3pt,tw}(t) - Z_V\left(\tilde{\partial}_t C_{V_0}^{3pt,tw}(t) + \tilde{q}_i C_{V_i}^{3pt,tw}(t)\right) = 0 + O(a^2) \quad (1)$$

$$\Delta^{W}(t) \equiv \delta m C_S^{3pt,W}(t) - Z_V\left(\tilde{\partial}_t C_{V_0}^{3pt,W}(t) + \tilde{q}_i C_{V_i}^{3pt,W}(t)\right) = 0 + O(a) \quad (2)$$

$$\Delta^{I}(t) \equiv \delta m C_S^{3pt,W}(t) - Z_V^{\text{imp}}\left(\tilde{\partial}_t C_{V_0}^{3pt,I}(t) + \tilde{q}_i C_{V_i}^{3pt,I}(t)\right) = 0 + O(a^2) \quad (3)$$

where $\delta m$ is the bare Wilson mass difference between the two valence flavours, $\delta\mu$ the twisted mass difference, and

$$C_{V_\mu}^{3pt,I}(t) = C_{V_0}^{3pt,W}(t) + ac_V\tilde{\partial}_\nu T_{\mu,\nu} \quad (4)$$

$$Z_V^{\text{imp}} = Z_V(1 + ab_V\bar{m}_q + a\bar{b}_V \operatorname{Tr} M). \quad (5)$$

This quantity can be measured easily to very high precision and without having to worry about excited states. Since it can be computed independently for each ensemble and then disappears in

the continuum limit, it is a very good probe for discretisation effects. However, in the Wilson case this is mostly sensitive to $b_V$, while the $c_V$ contribution disappears in the divergence because of (anti-)commutativity. This $b_V$ term is large because $b_V$ itself is 1 at tree level and $am_c$ is only moderately smaller than 1. One should also keep in mind that any observation about the lattice artefacts on this combination does not necessarily apply to each of its components individually.

The improvement coefficients are given as an input[16], but $b_V$ and $\bar{b}_V$ could also be determined from this data.

Note that, not only for the twisted mass case but also for the improved Wilson, the product $\delta m C_S^{3pt,W}$ is already $O(a)$ improved and does not need an explicit renormalisation[10]

The shape of those combinations of three-point functions are shown in Fig. 3 for one arbitrary choice of ensemble, and then Fig. 4 shows all ensembles, keeping only the central time slice. For both improved Wilson and twisted mass quarks, we observe an $a^2$ scaling for the three finest ensembles while higher orders play some role for the coarsest ensemble. The unimproved Wilson exhibits an extra $O(a)$ term, which we are able to fit given our high precision on $\Delta$ (this would be much less realistic on the final form factors).

Some results at higher masses are shown in Fig. 5, as $O(am_h^2)$ terms are expected.

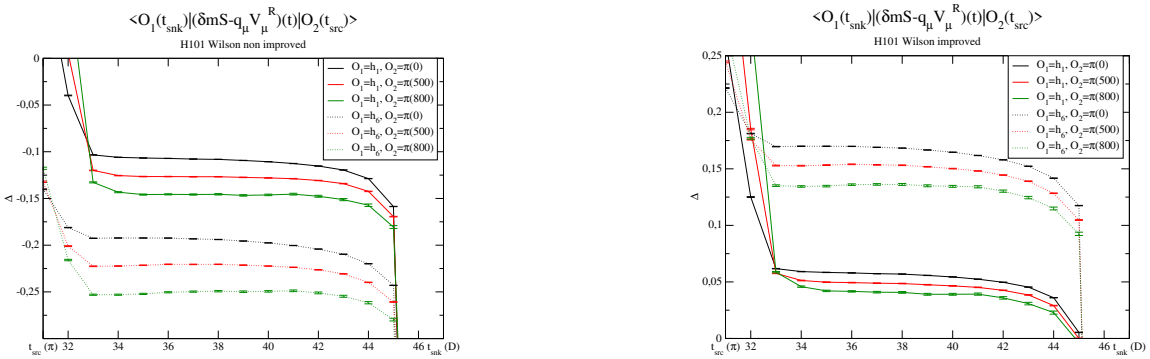


**Figure 3:** We show $\Delta^W(t)$ (left) and $\Delta^{tw}(t)$ (right) as a function of the time $t$ of the current insertion.

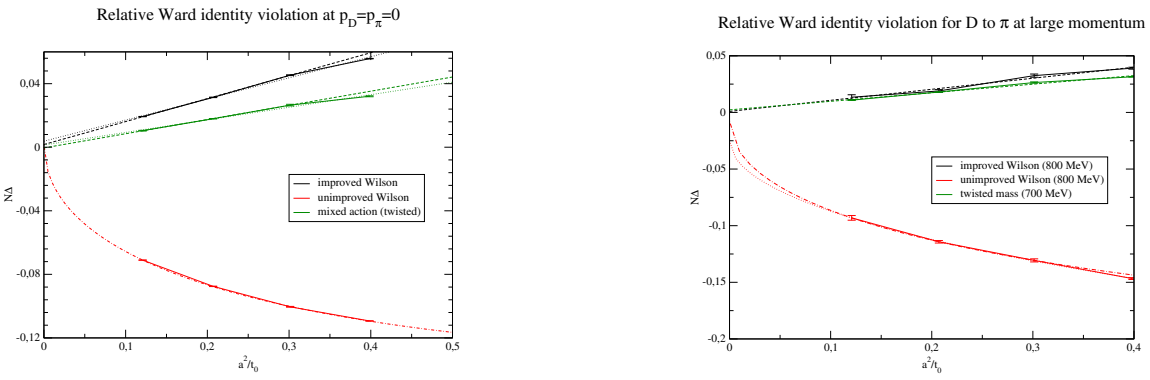


**Figure 4:** The y-axis is normalised by a factor $N$ such that the 2-norm of the 5 terms entering the Ward identity is fixed to 1. All those curves go to zero in the continuum but the intercept is not constrained a priori by our fitting formula.

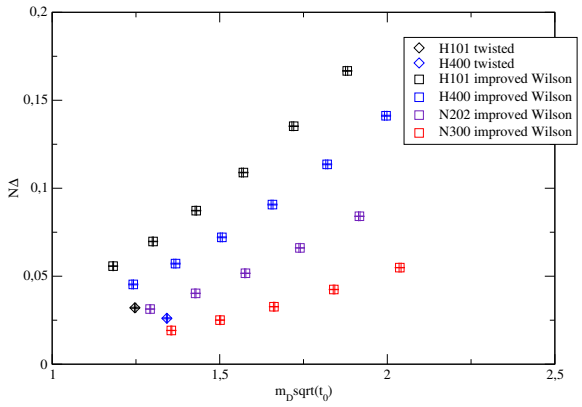


**Figure 5:** The Ward identity violations become larger as the heavy quark masses are higher (and similarly for larger momenta).

## 4. Extracting matrix elements

### 4.1 Combined fit

When computing matrix elements through three-point funtions, a well-known problem is that one needs a way to reliably estimate excited state contaminations. Our preferred method is a combined multi-exponential fit acting directly on the correlators:

$$C_\Gamma^{3pt}(t, t_{snk}) = \sum_{i=0}^{N_{\pi,max}} \sum_{j=0}^{N_{D,max}} p_{ij} e^{-E_i^\pi (t-t_{src})} e^{-E_j^D (t-t_{snk})} \tag{6}$$

$$C_\pi(t) = \sum_{i=0}^{N_{\pi,max}} \alpha_i e^{-E_i^\pi (t-t_{src})} \tag{7}$$

$$C_D(t) = \sum_{j=0}^{N_{D,max}} \beta_j e^{-E_j^D (t-t_{snk})}. \tag{8}$$

This choice avoids mixing various excited states into a derived ratio, avoids strong non-linearities in the model, and allows the gaussian approximation to make more sense, while using most of the available information.

In the typical case $N_{\pi,max} = N_{D,max} = 2$ so that this model has 12 parameters, but it is set dynamically as explained in sec. 4.2

### 4.2 Model average

Our model has many hyper-parameters: $N_{\pi,max}$, $N_{D,max}$, $t_{\Gamma,min}$, $t_{\Gamma,max}$, $t_{\pi,min}$, $t_{D,max}$, $t_{D,min}$, $t_{D,max}$. Our treatment of excited states only makes our estimate more reliable *if* we can have some knowledge of what the best values are for those hyper-parameters. We do this through a pseudo-Bayesian Model Average (pBMA) with the Akaike Information Criterion

$$AIC = \chi^2 + 2k, \tag{9}$$

where the number of parameters $k$ includes the implicit parameters of the cuts[11].

Our set of model is obtained by looping over some large range of values for all the hyper-parameters. This means $O(10k)$ models, which requires a non-negligible amount of computing time on a small cluster. Many of these models have a negligible weight and are therefore dropped before performing the bootstrap. Indeed a large number of bootstrap samples is also needed to get a precise covariance matrix, and we chose to use 2000.

Since we want the "true" model to be close enough to at least one model of our pBMA set, it is important to have a good control of the correlations. Indeed we observe that our data is very strongly correlated in time, as shown in Fig. 6.

Eventually, our bootstrap implementation means that for each boostrap sample $b$ we pick the result of model $i$ with probability

$$P(X_b = x_b^i) \propto e^{-AIC/2}. \tag{10}$$

The percentiles of the bootstrap distribution then provide an error bar which contains one contribution due to the statistical error and one contribution due to the systematic error, while being robust against outliers in this arbitrary probability distribution.

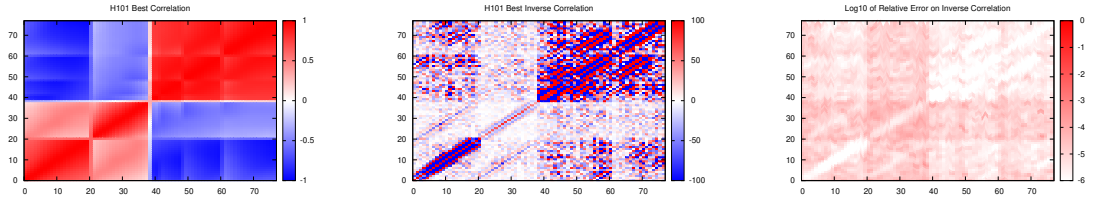


**Figure 6:** We show for one ensemble H101 -and the time intervals with lowest AIC- the correlation matrix (left), its inverse (middle), and the relative error on the inverse (right) obtained by a second level of bootstrapping. The largest relative error is 19% but almost all of them are around $10^{-5}$. This shows that, although the inverse is not easily interpretable by eye, it is known to high precision. One can also check that all the eigenvalues of the correlation here are far from zero. With our statistics, this remains true as long as the time intervals are not unreasonably long.

Some results are shown as an example in Fig. 7, which corresponds to the pBMA estimate of one matrix element for one choice of kinematics on one ensemble.

### 4.3 Ward Identities and Form Factor decomposition

The Ward identities on three-point functions can be promoted to a relation between matrix elements: the quantity

$$\Delta_{WI} = \delta m \langle S \rangle - \tilde{q}_\mu \langle \hat{V}_\mu \rangle \tag{11}$$

becomes zero in the continuum limit.

This is already encoded in the usual form factor decomposition:

$$< S > = (M_D^2 - M_P^2) f_0(q^2) \tag{12}$$

$$< \hat{V}_\mu > = \left[ P_\mu - q_\mu \frac{M_D^2 - M_P^2}{q^2} \right] f_+(q^2) + q_\mu \frac{M_D^2 - M_P^2}{q^2} f_0(q^2). \tag{13}$$

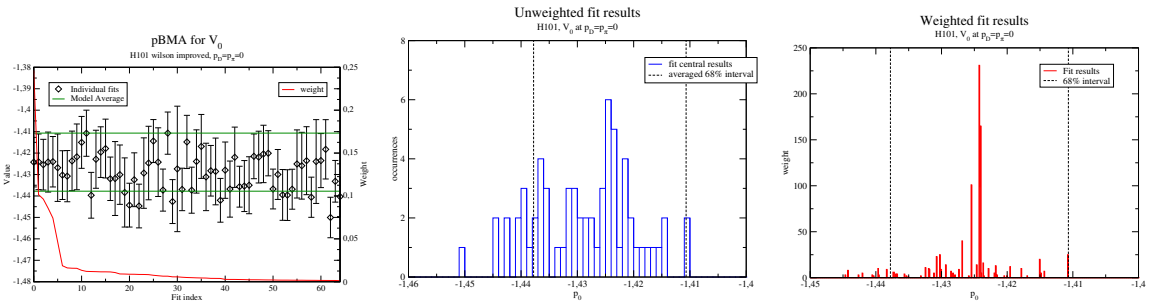


**Figure 7:** The individual fits and their pBMA are shown in the left panel, with fits ordered by Akaike weight. We also show histograms correspondings to the distribution of the central values of those individual fits, weighted (right) or not (centre).

Equation 11 cannot be checked at a precision similar to Eq. 3 but it provides an extra check sensitive to the correctness of our fits: the loss of control on excited states, either in the matrix elements or in the masses, would likely break Eq. 11.

Results are shown in Fig. 8 for the case $p_D = p_\pi = 0$, which is available on both the Wilson and the twisted calculations without any need for interpolations.

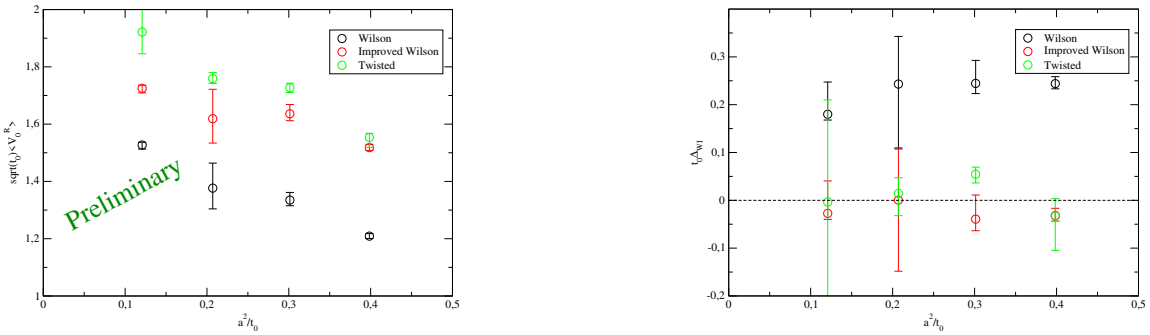


**Figure 8:** For the specific kinematics $D(p_D = 0) \to \pi(p_\pi = 0)$, we show the renormalised matrix elements (left) and the associated Ward identity violation Eq. 11 (right). In this particular case, this is equivalent to checking whether the form factors obtained from $\langle S \rangle$ and from $\langle V_0 \rangle$ are compatible. Points with larger errors mostly suffer from excited state uncertainties.

## 5. A quick look at the leptonics

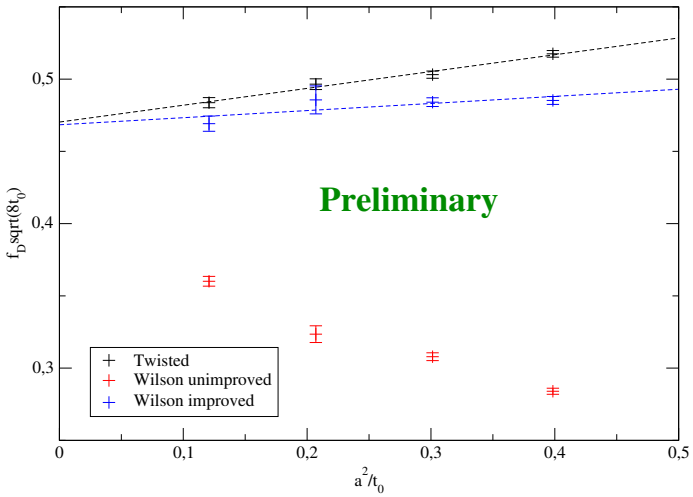


**Figure 9:** Using a subset of the data used in [12], we make a similar comparison of our actions in the case of the leptonic decays.

## 6. Conclusion

We presented two studies of heavy-light decays, with non-perturbatively $O(a)$-improved Wilson or with Wilson twisted mass quarks in the valence. We showed how a Ward identity can be used to assess scaling violations to high precision. The scaling of this quantity is consistent with our expectation of an $O(a^2)$ behaviour.

None of these two actions showed a clear superiority over the other one, in the range of quark masses and observables considered here. There is however a practical difference: in one case one needs to perform a matching of the quark mass parameters, but then the $O(a)$ improvement is automatic, while in the other case one has to compute extra improvement coefficients and the associated contractions for each observable.

We presented a set of techniques to extract matrix elements while controlling for excited state contributions. Eventually, the two discretisations agree in the continuum limit, and only depart from an $O(a^2)$ behaviour on the coarsest ensemble. A fifth CLS ensemble at $a = 0.039$ fm will soon allow this to be tested further, but currently this comparison is mostly limited by our statistics.

## References

[1] G. Herdoíza, C. Pena, D. Preti, J. Á. Romero and J. Ugarrio, EPJ Web Conf. **175** (2018), 13018 doi:10.1051/epjconf/201817513018 [arXiv:1711.06017 [hep-lat]].

[2] A. Bussone *et al.* [ALPHA], PoS **LATTICE2018** (2019), 270 doi:10.22323/1.334.0270 [arXiv:1812.01474 [hep-lat]].

[3] J. Ugarrio *et al.* [Alpha], PoS **LATTICE2018** (2018), 271 doi:10.22323/1.334.0271 [arXiv:1812.05458 [hep-lat]].

[4] A. Bussone *et al.* [ALPHA], PoS **LATTICE2018** (2019), 318 doi:10.22323/1.334.0318 [arXiv:1903.00286 [hep-lat]].

[5] J. Frison, A. Bussone, G. Herdoíza, C. Pena, J. Á. Romero and J. Ugarrio, PoS **LATTICE2019** (2019), 234 doi:10.22323/1.363.0234 [arXiv:1911.02412 [hep-lat]].

[6] A. Conigli, A. Bussone, J. Frison, G. Herdoiza, C. Pena, D. Preti, J. A. Romero and J. Ugarrio, PoS **LATTICE2021** (2022), 091 doi:10.22323/1.396.0091 [arXiv:2112.00666 [hep-lat]].

[7] J. Frison, G. Herdoiza, C. Pena, J. A. Romero and J. Ugarrio, PoS **LATTICE2021** (2022), 320 doi:10.22323/1.396.0320 [arXiv:2112.03047 [hep-lat]].

[8] A. Bussone, A. Conigli, G. Herdoiza, J. Frison, C. Pena, D. Preti, J. A. Romero, A. Saez and J. Ugarrio, PoS **LATTICE2021** (2022), 258 doi:10.22323/1.396.0258

[9] G. M. de Divitiis, R. Petronzio and N. Tantalo, Phys. Lett. B **692** (2010), 157-160 doi:10.1016/j.physletb.2010.07.031 [arXiv:1006.4028 [hep-lat]].

[10] T. Bhattacharya, R. Gupta, W. Lee, S. R. Sharpe and J. M. S. Wu, Phys. Rev. D **73** (2006), 034504 doi:10.1103/PhysRevD.73.034504 [arXiv:hep-lat/0511014 [hep-lat]].

[11] W. I. Jay and E. T. Neil, Phys. Rev. D **103** (2021), 114502 doi:10.1103/PhysRevD.103.114502 [arXiv:2008.01069 [stat.ME]].

[12] A. Conigli et al. , PoS **LATTICE2022**, 351

[13] G. M. de Divitiis, M. Guagnelli, R. Petronzio, N. Tantalo and F. Palombi, Nucl. Phys. B **675** (2003), 309-332 doi:10.1016/j.nuclphysb.2003.10.001 [arXiv:hep-lat/0305018 [hep-lat]].

[14] G. M. de Divitiis, M. Guagnelli, F. Palombi, R. Petronzio and N. Tantalo, Nucl. Phys. B **672** (2003), 372-386 doi:10.1016/j.nuclphysb.2003.09.013 [arXiv:hep-lat/0307005 [hep-lat]].

[15] D. Guazzini, R. Sommer and N. Tantalo, JHEP **01** (2008), 076 doi:10.1088/1126-6708/2008/01/076 [arXiv:0710.2229 [hep-lat]].

[16] A. Gerardin, T. Harris and H. B. Meyer, Phys. Rev. D **99** (2019) no.1, 014519 doi:10.1103/PhysRevD.99.014519 [arXiv:1811.08209 [hep-lat]].